

Intelligent maximum power point tracker enhanced by sliding mode control

Hussain Attia¹, Ahmad Elkhateb²

¹Department of Electrical, Electronics, and Communication Engineering (EEE), School of Engineering, American University of Ras Al Khaimah, Ras Al Khaimah, United Arab Emirates (UAE)

²School of Electronics, Electrical Engineering, and Computer Science, Queen's University, Belfast, United Kingdom

Article Info

Article history:

Received Aug 8, 2021

Revised Mar 10, 2022

Accepted Mar 28, 2022

Keywords:

ANN algorithm

DC-DC boost converter

MPPT

Photovoltaic PV cell

Sliding mode control SMC

ABSTRACT

In solar photovoltaic systems applications, the maximum power point tracker has been involved for different purposes to support their performance. The maximum power point tracking (MPPT) works on growing the obtained electricity from the solar photovoltaic energy and consequently increases the quantity of the delivered electrical power from the photovoltaic (PV) system. Relying on this point, this paper introduces an intelligent tracker to guarantee the MPP working condition for a small size 150 W stand-alone PV system. In this study, an intelligent algorithm is proposed to have a fast and accurate tracker. Moreover, a robust sliding mode controller is inserted for improving the performance of a direct current (DC-DC) boost converter. The converter is working in a continuous conduction mode operation to enhance the MPP tracker. Simulink of MATLAB is adopted to implement the system. The results of the simulated tracker are evaluated comparatively based on the artificial neural network (ANN) algorithm with and without inserting the sliding mode (SM) controller for different light intensity trends and levels. Simulation results analyzed and confirmed the effectiveness of the proposed tracker.

This is an open access article under the [CC BY-SA](https://creativecommons.org/licenses/by-sa/4.0/) license.



Corresponding Author:

Hussain Attia

Department of Electrical, Electronics, and Communication Engineering

American University of Ras Al Khaimah

Ras Al Khaimah, 10021, United Arab Emirates (UAE)

Email: hattia@aurak.ac.ae

1. INTRODUCTION

Solar energy advantages which are being clean, inexpensive, and ubiquitous make solar energy a very important source of renewable energy. Photovoltaic (PV) cell is the fundamental part of the PV module, which converts the solar photovoltaic energy to an electricity as a direct current (DC) voltage source. The power quantity is positively proportional to the instantaneous level of the incident light whereas it is negatively proportional with instantaneous level of PV panel temperature. The instantaneous harvested energy is converted to electrical power fluctuating based on the levels of light intensity and ambient temperature [1]–[3]. In the solar PV applications, to gain higher electrical power by solar energy conversion, many maximum power point tracking (MPPT) algorithms are explained in [4], whereas different algorithms and methods have been proposed and analyzed in [5]–[19]. Incremental conductance (IC), short circuit current, constant voltage (CV), and perturb & observe (P&O) algorithm have offered in [5]–[9] to maximize the power point tracking conditions during the work of the PV panel.

The demerits of the above MPPT algorithms are represented by low accuracy, low robustness, slow and oscillated response. The researchers are focusing on mitigating the effects of these demerits by proposing

higher performance algorithms and methods. Fuzzy logic control has presented in [10]–[16] for improving MPP tracking process in terms of better robustness and higher response. Fuzzy logic controller (FLC) with hill-climbing algorithm offered in [10] to have enhanced MPPT performance. A precise and quick response of fuzzy logic controller has been proposed through sensorless strategy in [11]. The effectiveness of the FLC controller is analyzed in [12]–[16] through studying membership effect on the stability behavior of the MPPT tracker for different purposes PV system.

Intelligent neural network-based algorithms have presented in [17]–[26] for multidisciplinary systems. Artificial neural network (ANN) algorithm guarantees the effective, fast, and accurate MPPT response. ANN-based controllers were proposed in [17]–[23], to select a suitable duty cycle of DC-DC converter. Neural network algorithms were proposed in [24]–[26] for other applications in terms of power factor correction.

On the other side, the researchers focused on analyzing the converter performance effect on PV system effectiveness. Different types of converters, have been studies, and analyzed in [27]–[30]. To have a stable and robust response from the converter, sliding mode controller (SMC) have been proposed in many studies [31]–[35] to guarantee the robustness and accuracy in the converter performance and to have constant load voltage during the source or load variation.

This paper presents a stand-alone PV system of power size 150 W controlled by an intelligent MPP tracker supported by a robust SMC. The inserted SM controller works on having a smooth, accurate, and robust response from the involved boost converter. This paper focuses on the intelligent tracker performance after inserting the SM controller, whereas the difficulties of SM controller design, such as the chattering drawback, and will be discussed in the future study. The remaining is being as: the selected PV panel behavior is shown in section 2. The design of ANN structure shown in section 3. Section 4 shows the design steps of the SM controller and demonstrates the proposed system diagram. Section 5 describes the system simulation and analyze the collected simulation results. Section 6 shows the conclusion points.

2. PHOTOVOLTAIC MODULE

This study selects the PV module type ELDORA 150P [36] of main specifications as shown in Table 1. The level of delivered power from the ELDORA 150P panel is positively proportional to the level of incident light, whereas the delivered power is negatively proportional to ambient temperature of the panel. The output power behavior of the PV cell is nonlinear with the output voltage variation. The electrical representation of the smaller PV unit is shown in Figure 1.

Table 1. Electrical parameters of ELDORA 150P panel

PV Panel Parameter	Parameters Value
Maximum Power, P_{max} (W)	150
Maximum Voltage, V_{max} (V)	17.85
Maximum Current, I_{max} (A)	8.41
Open Circuit Voltage, V_{oc} (V)	22.58
Short Circuit Current, I_{sc} (A)	8.7
Panel Efficiency (%)	15.09
Temperature Coefficients (T_c) of Power ($\%/^{\circ}\text{C}$)	-0.41

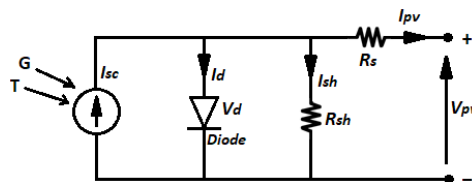


Figure 1. Electrical representation of a PV unit or cell

In (1) shows I_{pv} which is the output PV current, that equals the generated current I_{sc} minus diode current and minus shunt resistor R_{sh} current I_{sh} . From (2), the induced current I_{sc} can be calculated. The current value is related to the solar cell area A , the generation rate G_r , and the electron and hole diffusion lengths L_n , and L_p respectively. From (3), diode current I_d can be calculated, and from (4), the parallel current I_{sh} of the parallel resistor R_{sh} can be calculated. V_{pv} represents the output voltage of PV cell which is calculated from (5) by considering the drop voltage across the series resistor R_s . The total voltage out from the panel V_{pv_Module} and the current out from the panel I_{pv_Module} can be calculated from (6), and (7), respectively. The total output

voltage can be determined by considering the total serially connected solar units N_s , while the total current can be determined by considering the number of parallel-connected branches N_{sh} [9]–[13], [19]–[22]. The current and power delivered by the PV panel type ELDORA 150P are shown in Figure 2 including current curves in Figure 2(a) and power curves in Figure 2(b) at different levels of incident light; 200, 400, 600, 800, and 1000 W/m² at the normal temperature of the room 25 °C. Figure 3 shows the PV panel current curves in Figure 3(a) and power curves in Figure 3(b) at many ambient temperatures 15, 25, 35, 45, and 55 °C during a constant level of light intensity 1000 W/m².

$$I_{pv} = I_{sc} - I_d - I_{sh} \quad (1)$$

$$I_{sc} = qAG_r(L_n + L_p) \quad (2)$$

$$I_d = I_0 \left(e^{\frac{V_d}{V_T}} - 1 \right) \quad (3)$$

$$I_p = \frac{V_d}{R_{sh}} \quad (4)$$

$$V_{PV} = V_d - R_s I_{PV} \quad (5)$$

$$V_{pv_Module} = N_s x V_{PV} \quad (6)$$

$$I_{pv_Module} = N_{sh} x I_{PV} \quad (7)$$

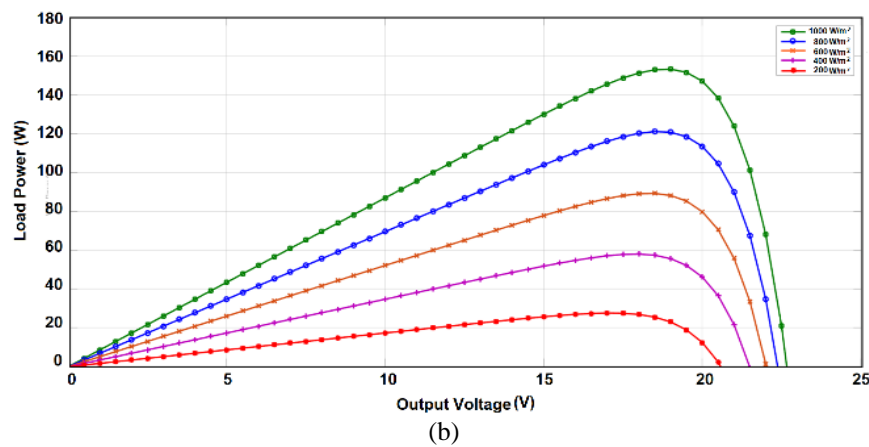
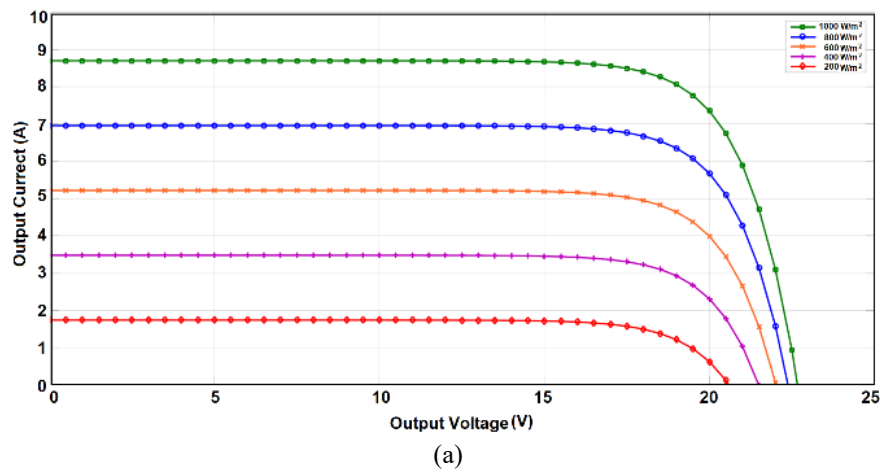


Figure 2. The behaviour of PV module type ELDORA 150P during different levels of light intensity and constant ambient temperature 25 °C (a) curves of output current and (b) curves of output power

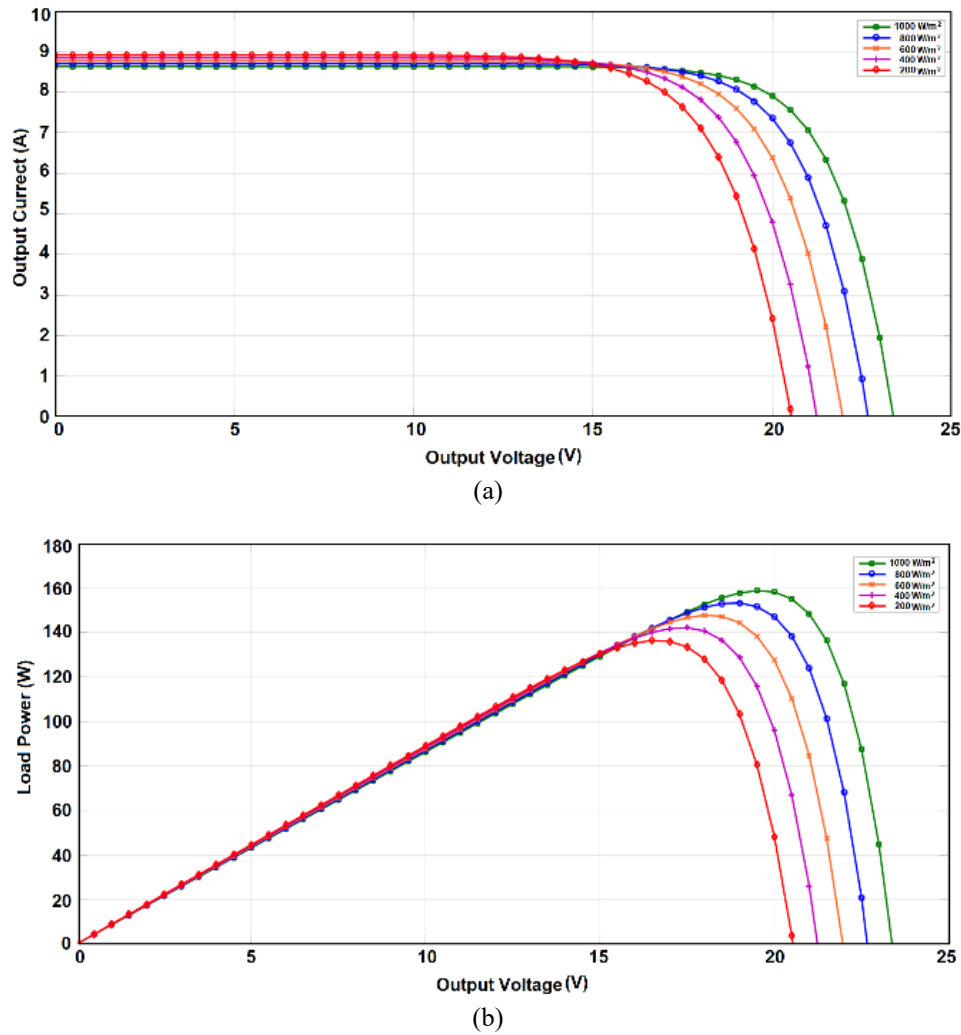


Figure 3. The behaviour of PV Module type ELDORA 150P during different levels of ambient temperature and fixed level of incident light 1000 W/m² (a) curves of output current and (b) curves of output power

3. ALGORITHM OF ARTIFICIAL NEURAL NETWORK

The characteristics of maximum power point tracker can be more accurate and fast in response using feed-forward ANN algorithm [17]–[26]. The neural network algorithm estimates the accurate value of the instantaneous MPP reference voltage by evaluating the instantaneous levels of the incident light and panel ambient temperature. A generated reference voltage enforces the involved boost converter to work in a MPP condition to harvest maximum power from the incident solar energy. Figure 4(a) explains the presented algorithm design of neural network. The ANN algorithm includes one, and two input layer, hidden layers respectively, and four neurons in each hidden layer. The output layer represents the last layer of the proposed ANN. The input layer receives the instantaneous values of light intensity and ambient temperature, whereas the output layer produces the instantaneous value of reference voltage after the processing of the hidden layer. Figure 4(b) shows the neuron structure, in which there are weights of each input to the neuron: X_{n1} , X_{n2} , X_{n3} , and X_{n4} . After weighting all neuron inputs, all together add to Bias (B) to produce the internal result of Z . One of activation functions (linear, sigmoidal, or hyperbolic transfer function) to produce the output value of y_n as shown in (8)–(11) respectively will manipulate the instantaneous produced value Z :

$$Z = \sum_{i=1}^N W_{ni} X_{ni} + \quad (8)$$

$$\text{Linear bipolar: } y_n = f(z) \quad (9)$$

$$\text{Sigmoidal: } f(z) = \frac{1}{1 + \exp^{-z}} \quad (10)$$

$$\text{Hyperbolic tan: } f(z) = \frac{1 + e^{-2z}}{1 - e^{-2z}} \quad (11)$$

The mean square error (MSE) is considered for evaluating the effectiveness of the presented NN algorithm. This parameter is demonstrated in (12), which indicates the difference between the target and predicted values. A smaller value of MSE indicates the accurate performance of the designed ANN algorithm.

$$MSE = \frac{1}{Q} \sum_{k=1}^Q \text{err}(k)^2 \quad (12)$$

Where Q is the input vectors number, and $\text{err}(k)$ is the error between the target and the estimated values.

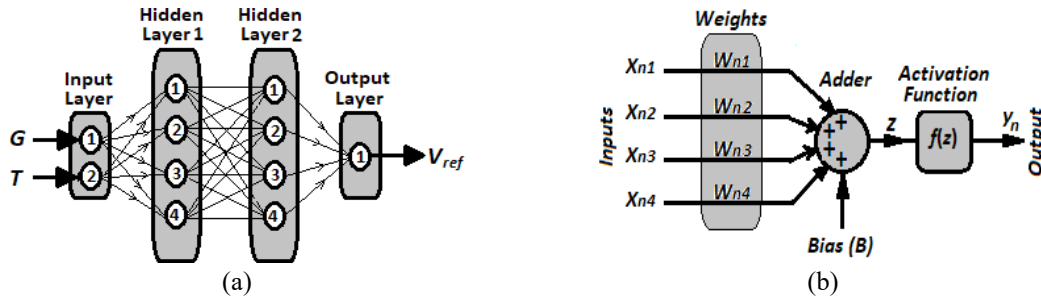


Figure 4. ANN Algorithm (a) the designed feed-forward ANN and (b) neuron structure

4. SLIDING MODE CONTROLLER DESIGN AND SYSTEM BLOCK DIAGRAM

The presented SMC design is suitable for DC-DC boost converters to remove the overshoot in the output load voltage by evaluating reference base voltage, the design of SMC starts from the dynamic (13) and (14) of the inductor current and output voltage variations with respect to time, as explained in Figure 5, which shows the power electronic circuit arrangement of DC-DC boost converter in Figure 5(a), the equivalent circuit when the insulated gate bipolar transistor (IGBT) is closed in Figure 5(b), and the equivalent circuit when the IGBT open in Figure 5(c) [31]–[35], [37].

$$\frac{di_L}{dt} = \frac{V_s}{L} - (1 - u) \frac{V_o}{L}$$

$$\frac{dV_o}{dt} = \frac{(1 - u)}{C} i_L - \frac{V_o}{RC}$$

Where the source voltage is represented by V_s , the converter inductance is represented by L , the converter capacitance is represented by C , and the load resistor is represented by R . The controller effectiveness is determined by evaluating the accuracy in determining the instantaneous switching state of u of the converter switch, and determining u formula started by determining the sliding surface S , then equaling S , and \dot{S} (the derivative of S) to zero. The sliding surface S is the summation of output voltage error ($e = x_1 = \text{reference voltage } V_{ref} - \text{output voltage } V_o$) and the derivative of the error ($x_2 = de/dt$):

$$S(x) = x_1 + x_2 \quad (13)$$

$$\text{So } S(x) = -\frac{1}{C} i_L + \left(\frac{1-RC}{RC}\right) V_o + V_{ref} \quad (14)$$

$$\text{And } \dot{S} = 0 = -\frac{1}{C} \left(\frac{V_s}{L} - (1 - u) \frac{V_o}{L}\right) + \left(\frac{1-RC}{RC}\right) \left(\frac{(1-u)}{C} i_L - \frac{V_o}{RC}\right) \quad (15)$$

A nonlinear component u_n , and an equivalent component u_{eq} are involved in u [31]–[34]:

$$u = u_{eq} + u_n \quad (16)$$

The formula of u_{eq} can be determined by equaling \dot{S} to zero:

$$u_{eq} = \frac{a_1 i_L + a_2 V_o - a_3 V_s}{a_1 i_L + a_3 V_o} \quad (17)$$

where

$$a_1 = \frac{1-RC}{RC^2} \quad (18)$$

$$a_2 = \frac{R^2 C + LRC - L}{LR^2 C^2} \quad (19)$$

$$a_3 = \frac{1}{LC} \quad (20)$$

Whereas the nonlinear component u_n is:

$$u_n = \text{sign}(S) \quad (21)$$

The presented intelligent MPP tracker supported by SMC is demonstrated as a block diagram in Figure 6. The selected PV panel ELDORA 150P is connected to the boost converter. The converter is controlled by the instantaneous value of u through the pulse width modulation (PWM) pluses generator. The ANN algorithm evaluates the variables of light intensity and ambient temperature for accurately producing a reference voltage. Enforcing the converter to be driven by reference voltage guarantees the MPP position to maximize harvesting the electricity through the PV panel. The designed sliding mode controller produces a suitable switching state u by monitoring the instantaneous reference voltage, output voltage and inductor current of the converter.

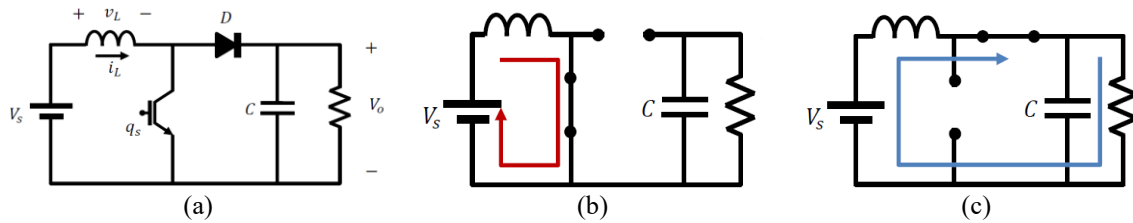


Figure 5. DC-DC boost converter (a) converter connection circuit, (b) the circuit at switch ON, and (c) the circuit at switch OFF

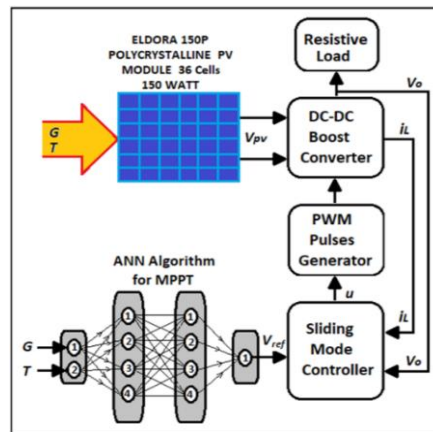


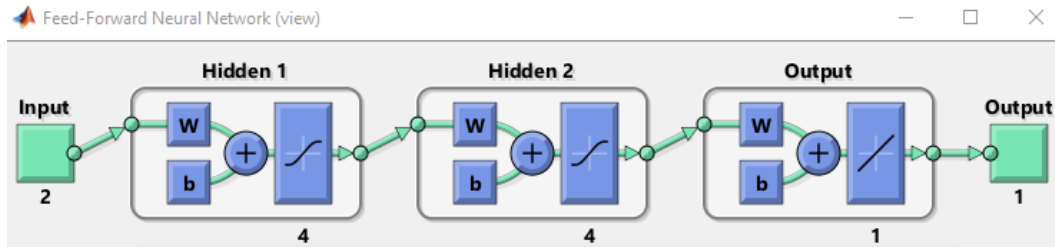
Figure 6. Diagram of the presented MPP tracker

5. SIMULATION RESULTS

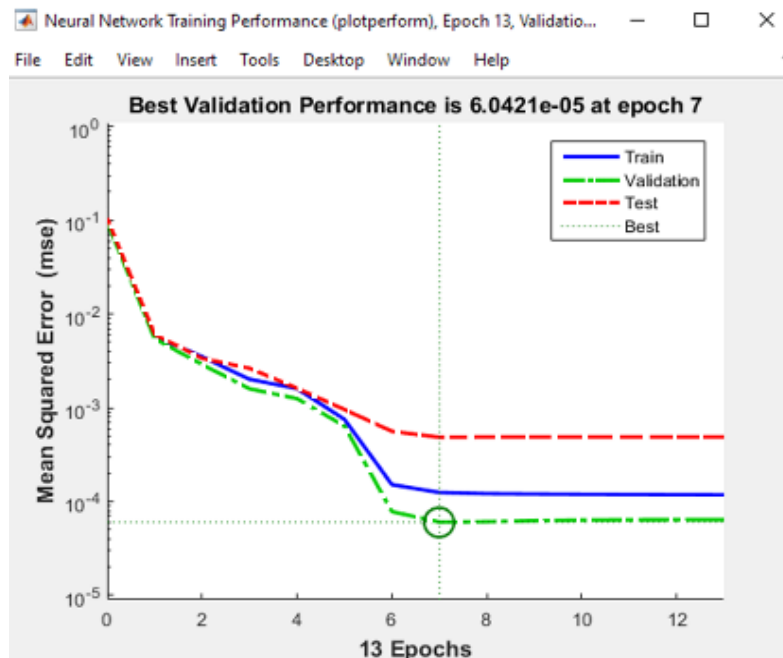
The boost converter parameters are designed by considering the study in [4], the selected switching frequency is 40 kHz, as shown in Table 2, in which the converter parameters are also shown. The study ANN involves input layer of two neurons, two hidden layers of four neurons each, and output layer of one neuron. Figure 7 shows the algorithm structure in Figure 7(a) and performance in terms of MSE in Figure 7(b) which reflects an accurate ANN performance of MSE (6.0421e-5) at epoch 7.

Table 2. Designed parameters of boost converter

Converter Parameter	Parameter Value
Inductor (mH)	10
Capacitor (μF)	2200
Connected load (Ω)	15
Switch frequency f_s (kHz)	40
Sampling time (μsec)	0.5



(a)



(b)

Figure 7 ANN algorithm (a) structure and (b) performance MSE

Figure 8 represents the full simulation program, which includes two simulations. The left part is for simulation of MPP tracker using ANN only, whereas the right position is for MPP tracker using ANN supported by the presented SM controller. The simulation results are collected during 1 second of four equally divisions 0.25 second. The simulation is done in a comparative way using ANN algorithm with and without the SMC inserting to evaluate the effectiveness of the SM controller in smoothing the mitigating the overshoot in the load power. Simulation results are collected during ambient room temperature 25 °C and different light intensity levels; 600, 800, 1000, and 700 W/m² respectively. Figure 9(a) shows the MPP tracker performance based on ANN only. The figure demonstrates the voltage, current, and power of the connected load. Overshoots are clearly noticed in the voltage, current, and power of the load. On the other hand, the positive effect of SM controller in smoothing the shape of load power is noticed in Figure 9(b), which shows the MPP tracker performance when it is supported by sliding mode controller, and all the overshoots are avoided. Figure 10 shows the tracker response in a comparative way before and after inserting the SMC and how the overshoots (red color) can be smoothed (blue color) by the inserted SM controller.

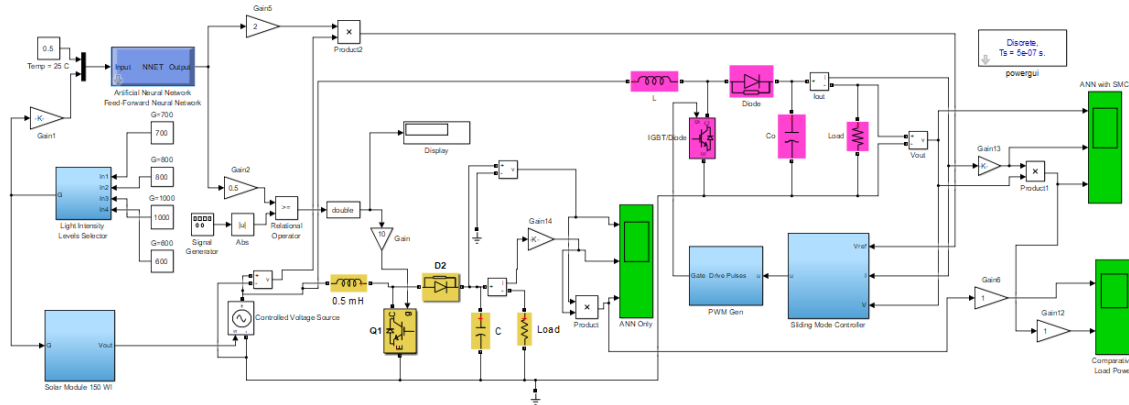


Figure 8. Presented intelligent MPP tracker simulation using ANN without and with SMC

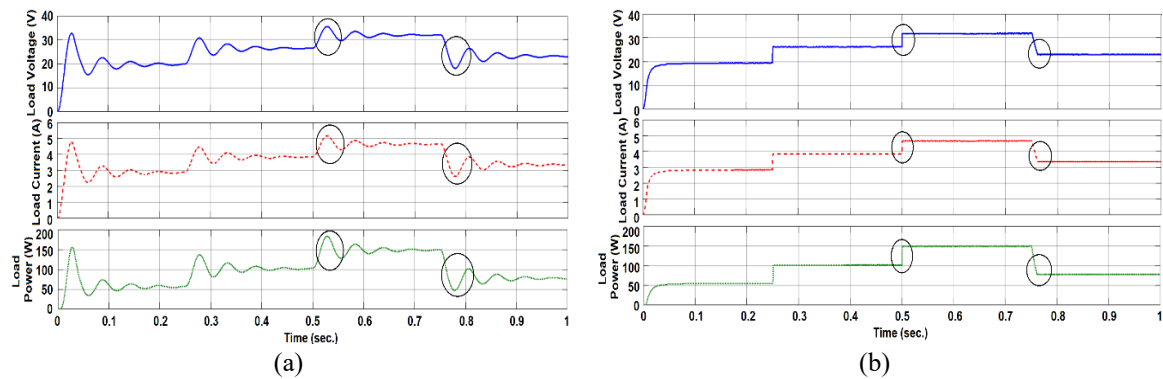


Figure 9. Presented tracker performance (a) using neural network algorithm only and (b) using ANN supported by SMC

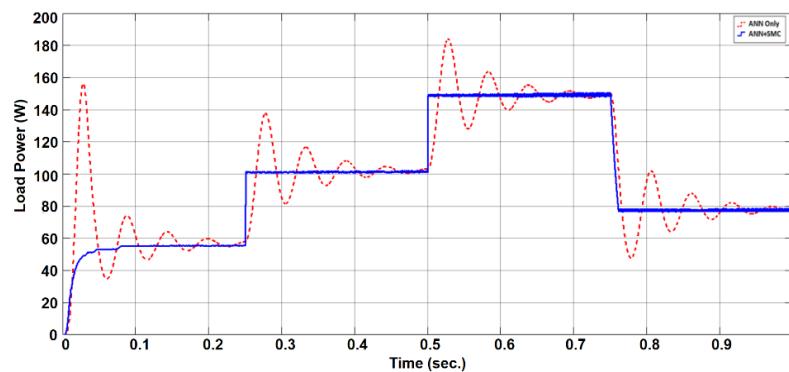


Figure 10. Load power comparison between tracker performances based on ANN without and with SMC

6. CONCLUSION

In this study, an intelligent MPP tracker supported by a robust sliding mode controller has been presented. The designed SM controller is suitable for boost converter. An intelligent tracker is evaluated comparatively with and without inserting SM controller. ANN algorithm has been adopted in this study to guarantee the MPP tracking working conditions through fast predicting an accurate reference voltage, and then this voltage has processed by the SM controller to have a smooth response from the tracker and to avoid the overshoot in the load power. Simulink of MATLAB is adopted to simulate the presented intelligent MPP tracker, firstly, and the simulation results are collected without inserting the SM controller into the tracker system. After that, the designed SM controller has inserted to support and enhance the tracker performance. The results

indicate the effectiveness of the presented MPP tracker after inserting the SM controller and promise a high-performance prototype as a future step.

ACKNOWLEDGEMENTS

H. Attia appreciates the financial support provided by the American University of Ras Al Khaimah–UAE, <https://aurak.ac.ae>. The work of A. Elkhateb was supported in part by the UK Engineering and Physical Sciences Research Council (EPSRC) under Grant EP/T026162/1.




REFERENCES

- [1] W. Obaid, Abdul-Kadir Hamid, and C. Ghenai, "Solar/wind pumping system with forecasting in Sharjah, United Arab Emirates," *International Journal of Electrical and Computer Engineering (IJECE)*, vol. 11, no. 4, pp. 2752–2759, August 2021, doi: 10.11591/ijece.v11i4.pp2752-2759.
- [2] T. K. S. Reddy and N. A. Rahim, "Photovoltaic inverter topologies for grid integration applications," *Advances in solar photovoltaic power plants*. Springer, Berlin, Heidelberg, June 2016, pp 13–42, , doi: 10.1007/978-3-662-50521-2_2
- [3] B. D. E. Mahdi, H. Abdelatif, and M. A. Zafrane, "An interactive approach for solar energy system: design and manufacturing," *International Journal of Electrical and Computer Engineering (IJECE)*, vol. 10, no. 5, pp. 4478–4489, October 2020, doi: 10.11591/ijece.v10i5.pp4478-4489.
- [4] D. C. K. Reddy, S. Satyanarayana, and V. Ganesh, "Design of hybrid solar wind energy system in a microgrid with MPPT techniques," *International Journal of Electrical and Computer Engineering (IJECE)*, vol. 8, no. 2, pp. 730–740, April 2018, doi: 10.11591/ijece.v8i2.pp730-740.
- [5] L. Rajan and R. Pradeep, "Performance Analysis of Maximum Power Point Tracking based Photovoltaic Module with Cuk Converter for Electrical Applications," *International Journal of Innovative Research in Electrical, Electronics, Instrumentation and Control Engineering (IJIREICE)*, vol. 1, no. 1, pp. 20–25, June 2013.
- [6] T. Noguchi, S. Togashi, and R. Nakamoto, "Short-current pulse-based maximum-power-point tracking method for multiple photovoltaic-and-converter module system," in *IEEE Transactions on Industrial Electronics*, vol. 49, no. 1, pp. 217–223, February 2002, doi: 10.1109/41.982265.
- [7] H. Attia and S. Ulusoy, "A new Perturb and Observe MPPT Algorithm based on two steps variable voltage control," *International Journal of Power Electronics and Drive Systems (IJPEDS)*, vol. 12, no. 4, pp. 2201–2208, December 2021, doi: 10.11591/ijpeds.v12.i4.pp2201-2208.
- [8] A. Touati, E. Abdelmounim, M. Aboulfatah, A. Moutabir, and R. Majdoul, "Improved strategy of an MPPT based on the torque estimator for variable speed turbines," *International Review on Modelling and Simulations (IREMOS)*, vol 8, no. 6, pp. 620–631, 2015, doi: 10.15866/iremos.v8i6.7122.
- [9] A. Youcef, A. Miloudi, R. Sayah, and H. Sayah, "Optimization of partially shaded PV array using a modified P&O MPPT algorithm," *Leonardo Electronic Journal of Practices and Technologies*, vol. 15, no. 28, pp. 179–196, January–June 2016.
- [10] B. N. Alajmi, K. H. Ahmed, S. J. Finney, and B. W. Williams, "Fuzzy-Logic-Control Approach of a Modified Hill-Climbing Method for Maximum Power Point in Microgrid Standalone Photovoltaic System," in *IEEE Transactions on Power Electronics*, vol. 26, no. 4, pp. 1022–1030, April 2011, doi: 10.1109/TPEL.2010.2090903.
- [11] M. El Azaoui, H. Mahmoudi, and K. Boudaraia, "Sensorless fuzzy MPPT technique of solar PV and DFIG based wind hybrid system," *International Review on Modelling and Simulations (IREMOS)*, vol. 10, no. 3, pp. 152–159, June 2017, doi: 10.15866/iremos.v10i3.11361.
- [12] K. H. Chlok, M. F. Tajuddin, T. S. Babu, S. M. Ayob, T. Sutikno, "Optimal extraction of photovoltaic energy using fuzzy logic control for maximum power point tracking technique", *International Journal of Power Electronics and Drive System (IJPEDS)*, vol. 11, no. 3, pp. 1628–1639, September 2020, doi: 10.11591/ijpeds.v11.i3.pp1628-1639.
- [13] L. Farah, A. Haddouche, and A. Haddouche, "Comparison between proposed fuzzy logic and ANFIS for MPPT control for photovoltaic system," *International Journal of Power Electronics and Drive System (IJPEDS)*, vol. 11, no. 2, pp. 1065–1073, June 2020, doi: 10.11591/ijpeds.v11.i2.pp1065-1073.
- [14] B. B. Krishnan, V. Ganapathy, S. A. Priya, and C. N. Kumar, "Design and implementation of FPGA based fuzzy controller for VIENNA rectifier," *International Review on Modelling and Simulations (IREMOS)*, vol. 7, no. 3, pp. 387–393, June 2014, doi: 10.15866/iremos.v7i3.912.
- [15] I. Abadi, A. Musyafa, and A. Soeprijanto, "Design and implementation of active two axes solar tracking system using particle swarm optimization based fuzzy logic controller," *International Review on Modelling and Simulations (IREMOS)*, vol. 8, no. 6, pp. 640–652, 2015, doi: 10.15866/iremos.v8i6.7907.
- [16] A. H. El Khateb, N. Abd. Rahima, and J. Selvaraja, "Fuzzy logic control approach of a maximum power point employing SEPIC converter for stand-alone photovoltaic system," *Procedia Environmental Sciences*, vol. 17, pp. 529–536, 2013, doi: 10.1016/j.proenv.2013.02.068.
- [17] S. Assahout, H. Elaisaoui, A. El Ougli, B. Tidhaf, and H. Zrouri, "A neural network and fuzzy logic based MPPT algorithm for photovoltaic pumping system," *International Journal of Power Electronics and Drive System (IJPEDS)*, vol. 9, no. 4, pp. 1823–1833, December 2018, doi: 10.11591/ijpeds.v9.i4.pp1823-1833.
- [18] H. Attia and K. Hossin, "Hybrid technique for an efficient PV system through intelligent MPPT and water cooling process," *International Journal of Power Electronics and Drive System (IJPEDS)*, vol. 11, no. 4, pp. 1835–1843, December 2020, doi: 10.11591/ijpeds.v11.i4.pp1835-1843.
- [19] A. Ibnelouad, A. Elkari, H. Ayad, and M. Mjahed, "A neuro-fuzzy approach for tracking maximum power point of photovoltaic solar system," *International Journal of Power Electronics and Drive Systems (IJPEDS)*, vol. 12, no. 2, pp. 1252–1264, June 2021, doi: 10.11591/ijpeds.v12.i2.pp1252-1264.
- [20] N. Kalaierasi, S. Paramasivam, and S. Kundu, "Control of Z-source inverter based PV system with MPPT using ANFIS," *International Review on Modelling and Simulations (IREMOS)*, vol. 7, no. 5, pp. 797–806, 2014, doi: 10.15866/iremos.v7i5.1970.
- [21] H. Attia and K. Hossin, "Integrated Renewable PV System through Artificial Neural Network Based MPPT and Water Cooling Treatment," *2019 International Conference on Electrical and Computing Technologies and Applications (ICECTA)*, 2019, pp. 1–5, doi: 10.1109/ICECTA48151.2019.8959581.




- [22] D. Mathur, "Maximum Power Point Tracking with Artificial Neural Network," *International Journal of Emerging Science and Engineering (IJESE)*, vol. 2, no. 3, pp. 38-42, January 2014.
- [23] R. Haque, "Transmission loss allocation using artificial neural networks," Doctoral dissertation, University of Saskatchewan Saskatoon, Canada, March 2006. [Online]. Available: <https://citeseerx.ist.psu.edu/viewdoc/download?doi=10.1.1.906.3053&rep=rep1&type=pdf>.
- [24] R. Rao and S. S. Dash, "Power quality enhancement by unified power quality conditioner using ANN with hysteresis control", *International Journal of Computer Applications*, vol. 6, no. 1, pp. 9-15, September 2010, [Online]. Available: <https://citeseerx.ist.psu.edu/viewdoc/download?doi=10.1.1.206.4810&rep=rep1&type=pdf>.
- [25] H. Attia, "A new intelligent power factor corrector for converter applications," *6th International Conference on Control, Modeling and Computing (CMC 2020)*, July 2020, Toronto, Canada, doi: 10.5121/csit.2020.100915.
- [26] H. Attia, M. Al Zarooni, and A. Cazan, "Ultrasonic Frequency Inverter for Piezoelectric Transducer Driving: The Negative Effects on Grid and the Intelligent Solution," *2019 International Conference on Electrical and Computing Technologies and Applications (ICECTA)*, 2019, pp. 1-5, doi: 10.1109/ICECTA48151.2019.8959609.
- [27] C. P. Basso, *Switch-Mode Power Supplies Spice Simulations and Practical Design*, McGraw-Hill Education, 2008.
- [28] D. Sattianadan, G. R. P. Kumar, R. Sridhar, K. V. Reddy, B. S. U. Reddy, and P. Mamatha, "Investigation of low voltage DC microgrid using sliding mode control," *International Journal of Power Electronics and Drive System (IJPEDS)*, vol. 11, no. 4, pp. 2030-2037, September 2020, doi: 10.11591/ijpeds.v11.i4.pp2030-2037.
- [29] C. S. Purohit, M. Geetha, P. Sanjeevikumar, P. K. Maroti, S. Swami, and V. K. Ramachandaramurthy, "Performance analysis of DC/DC bidirectional converter with sliding mode and pi controller," *International Journal of Power Electronics and Drive System (IJPEDS)*, vol. 10, no. 1, pp. 357-365, March 2019, doi: 10.11591/ijpeds.v10.i1.pp357-365.
- [30] G. R. Walker and P. C. Sernia, "Cascaded DC-DC converter connection of photovoltaic modules," in *IEEE Transactions on Power Electronics*, vol. 19, no. 4, pp. 1130-1139, July 2004, doi: 10.1109/TPEL.2004.830090.
- [31] H. Guldemir, "Sliding Mode Control of Dc-Dc Boost Converter," *Journal of Applied Sciences*, vol. 5, no. 3, pp. 588-592, 2005, doi: 10.3923/jas.2005.588.592.
- [32] F. Tahri, A. Tahri, and S. Flazi, "Sliding Mode Control for DC-DC Buck Converter," *Conference: Third International Conference on Power Electronics and Electrical Drives ICPEED'14*, December 2014, doi: 10.13140/2.1.1857.4408.
- [33] H. Guldemir, "Modeling and Sliding Mode Control of Dc-Dc Buck-Boost Converter," *6th International Advanced Technologies Symposium (IATS'11)*, vol. 4, pp. 475-480, May 2011, [Online]. Available: <https://zdocs.ro/doc/dc-dc-buckdc-buck-boost-converter-80pzw398w0po>.
- [34] I. Trushev, N. Mastorakis, I. Tabahnev, and V. Mladenov, "Adaptive Sliding Mode Control for DC/DC Buck Converters," *WSEAS Transactions on Electronics*, vol. 2, no. 4, pp. 109-113, October 2005, [Online]. Available: <https://www.researchgate.net/publication/234806929>.
- [35] K. B. Saad, A. Sahbani, and M. Benrejeb, "Sliding mode control and fuzzy sliding mode control for DC-DC converters," *Sliding Mode Control*, pp. 1-24, April 2011, doi: 10.5772/15151.
- [36] Vikramsolar, "Vikram Solar Limited 'The Chambers'," 8th Floor, 1865, Rajdanga Main Road, Kolkata-700107, West Bengal, India [Online]. Available: <https://www.vikramsolar.com/wp-content/uploads/2016/04/ELDORA-150P-Micro-Series-1.pdf>.
- [37] D. W. Hart, *Power Electronics*, Tata McGraw-Hill Education, New York, Americas, 2011.

BIOGRAPHIES OF AUTHORS



Hussain Attia    earned his Ph.D. degree in power electronics from University of Malaya, Kuala Lumpur, Malaysia, and M.Sc. degree in electronic engineering from the University of Technology, Baghdad, Iraq. Currently, he is working as a faculty member in Department of Electrical, Electronics and Communications Engineering at American University of Ras Al Khaimah, Ras Al Khasimah, UAE. He served as a technical and organizing member for many IEEE and international conferences such as ICEDSA/2016, ICECTA/2017, ICEWES/2018, and ICECTA/2019. Hussain's research interests include power electronics, AC and DC drives, PWM inverters (single phase and three phases), harmonics reduction techniques, and intelligent control. He can be contacted at email: hattia@aurak.ac.ae.



Ahmad Elkhateb    is a Senior Lecturer in power electronics with the School of Electronics, Electrical Engineering, and Computer Science (EEECS), Queen's University, Belfast, United Kingdom. His main research interests include power electronics, DC/DC converters, power generation, control, and implementation of power converters for the integration of renewable energy resources. Elkhateb is a senior member of IEEE, a full college member of the EPSRC and associate editor for the IET power electronics journal. He was the local organising chair for the ISSC 2018 conference and a member of the national organising committee for the 5th IFAC conference ICONS 2019. He can be contacted at email: A.Elkhateb@qub.ac.uk.